

Initial Results of Magnetotelluric Array Surveying at the Dixie Valley Geothermal Area, with Implications for Structural Controls and Hydrothermal Alteration

Philip E. Wannamaker
University of Utah/Energy & Geoscience Institute
423 Wakara Way, Suite 300
Salt Lake City, UT 84108
pewanna@egi.utah.edu

Key words: Dixie Valley, Basin and Range, geophysics, magnetotellurics, hydrothermal alteration.

ABSTRACT

A new-generation MT array measurement system was applied in a contiguous bipole deployment at the Dixie Valley thermal area. Basic goals of the survey are 1), resolve a fundamental structural ambiguity at the Dixie Valley thermal area (single range-front fault versus shallower, stepped pediment; 2), delineate fault zones which have experienced fluid flux as indicated by low resistivity; 3), image the disposition of resistive, possible reservoir formations in the subsurface; and 4), from a generic standpoint, investigate the capability of fully sampled electrical data for resolving subsurface structure. MT surveying using a remote reference was carried out on three, 4-6 mile long profiles totalling 14 line miles, each crossing the Stillwater fault zone approximately at right angles, over the frequency range of 10 kHz to 0.03 Hz. These lines cross the Senator Fumeroles area, the Cottonwood Creek and main producing area, and the low-permeability region through the section 10-15 area. Initial 2-D inversion suggests that shallow pediment basement rocks extend for a considerable distance (~1-1/2 km) southeastward from the topographic scarp of the Stillwater Range. A particularly low resistivity zone flanks the interpreted main offsetting fault and may be due to alteration from geothermal fluid outflow and upflow.

Introduction

Predictive capability for subsurface resource location is an important aspect of a geothermal exploration tool. Geophysical methods have long received attention for this purpose due to their ability to provide structural images of the underground from data taken at the surface. Of the various physical properties of the earth, electrical resistivity is one which can be strongly affected by geothermal processes. Since an increased fluid content due to fracturing, and the development of more conductive alteration minerals (clays, etc.), can give rise to an electrical resistivity contrast, electromagnetic (EM) methods of probing have been investigated and applied for many years. The reliable mapping of electrical resistivity should increase chances of discovering blind geothermal resources, in defining the extent of geothermal reservoirs, in imaging controlling structures for geothermal systems, and in locating and characterizing permeable fracture zones.

However, images of subsurface resistivity have suffered in resolution due to limited data type, inadequate data sampling, and non-optimal inversion approaches translating data to models. We have applied a new-generation array magnetotelluric (MT) system in a contiguous bipole deployment over three profiles at the Dixie Valley thermal area (Figure 1). This well-sampled data set is being analysed using a new inversion algorithm for MT image construction

Wannamaker

based on stabilization using a-priori constraints. One of our overall goals is to provide better tools, methods and data for resource identification and characterization using electromagnetic methods. A specific goal of the survey is to resolve a fundamental structural ambiguity at the Dixie Valley thermal area (single rangefront fault versus shallower, stepped pediment).

Geological Background

The Dixie Valley geothermal field lies in a highly extended area of northwestern Nevada within the Battle Mountain heat flow high and fields of Late Cenozoic volcanism (Blakely, 1988; Christiansen and Yeats, 1992). Modern cumulative extension rate in the western Great Basin is nearly 1 cm/yr, with a concentration of such in the Central Nevada Seismic Belt within which Dixie Valley lies (Bennett et al., 2003). The Dixie Valley field has been considered a classic rangefront fault system with production mainly from brittle igneous units represented by Oligocene silicic volcanics, Cretaceous granodiorite, or Jurassic mafic rocks (spilite or ophiolite) (Okaya and Thompson, 1985; Waibel, 1987; Dilek and Moores, 1995), possibly promoted by favorable stress regimes and fault orientations (Barton et al., 1998; Hickman et al., 1998). The thermal anomaly is interpreted in terms of deep circulation (Blackwell et al., 2000), although other geothermal systems toward the province margins show a clustering of magmatic helium isotope values (Welhan et al., 1988).

Controversy has arisen regarding the basic structural controls for the Dixie Valley system, as summarized in Figure 2. The traditional model has been one of a single normal fault dipping $\sim 55^\circ$ to the southeast connecting from the range/valley topographic contact through the producing wells (Benoit, 1999). However, recent drilling, gravity and thermal modeling in the Section 10-15 fumeroles area indicates a more complicated structural setting with the range-valley contact being a series of step-down faults under the pediment (Blackwell et al., 2000). Numerous normal faults are mapped in the Stillwater Range itself (Plank, 1999), some of which must provide controls on fluid flow for alteration and fumerole activity near the rangefront. Smith et al. (2001) also interpret Dixie Valley to be a nested graben structure with a relatively narrow, deep central section. An assessment of the multi-fault model, and the possible manifestation of fluid flow on one or more cryptic fault strands towards the Stillwater Range, is a principal goal of this project.

Field Acquisition and Processing Procedures

With array MT data, complete lateral sampling of the response is achieved through contiguous bipole deployment (Torres-Verdin and Bostick, 1992). The system currently being fielded possesses 60 recording channels, two-thirds of which typically are assigned to the electric field component across assumed strike (transverse magnetic or TM mode), one-third to the E-field along strike (transverse electric or TE mode), and a pair of magnetic field coils near the center of the deployment. In such a deployment, near-surface “static” distortions do not require qualitative correction (e.g., Pellerin and Hohmann, 1990) but instead are included directly in the inversion process. It is anticipated that the 2-D assumption is expected to hold reasonably well at least for the upper 2-3 km or the study area, aided by experience in understanding relative effects of finite strike upon the various tensor data subsets (summarized in Wannamaker, 1999).

MT signals are small in amplitude and require careful processing to achieve accurate

response functions. Some EM interference is generated by the existing power facility, but a distant remote reference synchronized by GPS timing was emplaced to suppress this through unbiased stacking. The overall time series processing comprised three main steps, generally as described by Larsen et al. (1996). First, the entire series is Fourier transformed to allow ultra-narrow band removal of spectral outliers such as 60 Hz and its harmonics. Second, the remaining time series is subdivided into short time segments with spectral estimates of each made using cascade decimation. Multiple coherence of spectral estimates between the base readings and the remote reference were made and low coherence time series segments rejected. Finally, the surviving spectral cross products undergo robust outlier removal following Egbert and Booker (1986).

Our approach to the inversion of array MT data to yield resistivity cross sections is based on the a-priori, maximum likelihood estimates of Tarantola (1987) and utilizes the finite element platform of DeLugao and Wannamaker (1996). The approach applies just the smoothing implicit in the a-priori step estimate unlike the explicit smoothing of other EM inversion efforts (e.g., DeGroot-Hedlin and Constable, 1990; Rodi and Mackie, 2001). The a-priori damping factor is updated each iteration to achieve stabilization in terms of fundamental parameter correlations characteristic of the physics of diffusive EM (e.g., conductivity-dimension) rather than brute-force suppression of spatial derivatives. Also, the parameters defining the image grow both laterally and vertically with depth, thereby preserving the influence of individual parameters at the surface according to basic EM scaling, and thus stabilizing the parameter step matrix and increasing depth of exploration.

Example Observed Data and Inversion Cross Section

This is a new data set and interpretation is in progress. So far, analysis has been carried out for the northerly line across the Senator fumaroles and Caithness geothermal wells 38-32 and 82-5 (Figure 1). The apparent resistivity and impedance phase pseudosections for both the transverse electric (TE, electric field along assumed NE-SW strike) and transverse magnetic (TM, electric field across assumed strike) are shown in Figure 3. For both modes, low apparent resistivities are characteristic of the eastern half of the profile for all frequencies over the thickest section of Dixie Valley graben sediments. Over the western half, low apparent resistivities occur at the higher frequencies, but an increase in this quantity in both modes (especially the TE) towards the lower frequencies is evident. The behavior is accompanied by impedance phase values falling below 45°. This indicates the shallowing of resistive basement in the westerly direction. Both modes are nearly isotropic until resistive basement begins to influence the data.

To quantify resistivity structure below the profile, the afore-described inversion algorithm was applied. Since the interpretation is taking place within a two-dimensional framework, inaccuracies from possible 3-D effects were reduced by emphasizing inversion of the TM mode over the whole frequency range, and the TE mode down to 3 Hz where the resistive basement becomes influential (Wannamaker, 1999). The starting model was consistent with regional MT surveying in the tectonically active eastern Great Basin (Wannamaker et al., 1997), with a smooth variation ~100 ohm-m down to 3 km depth, reaching 300 ohm-m near 10 km, and finally dropping to ~10 ohm-m below 20 km.

High resistivities (~1000 ohm-m) are seen under the Stillwater Range below 500 m depth and extending to the southeast under the pediment. Moderately high values (~100 ohm-m) persist

Wannamaker

at rather shallow depths (~400 m) from the topographic scarp where Senator fumaroles are located to a distance of about 1-1/2 km southeast just past well 38-32. Values of 100 ohm-m are more consistent with rock than alluvium (e.g., Ward et al., 1978), although alteration of the rock is a possibility. The alluvium of the main part of Dixie Valley is moderately conductive (10-25 ohm-m) in the upper 400 m, and quite conductive in the 500-1000 m depth range (< 3 ohm-m). A low resistivity limb dips upward from ~1 km depth to the near-surface under well 38-32 near the west flank of Dixie Valley. Senator fumaroles itself does not exhibit a strong resistivity expression.

Discussion and Conclusions

Lateral sampling uncertainties in MT are removed by the contiguous bipole deployment, which helps to maximize the resolution of resistivity structure. Remote referencing and robust processing have generally yielded very high quality data even in a field where power production has already been established. The inversion to date suggests that shallow basement rocks extend for a considerable distance to the SE before plunging steeply down the main range-front fault. It thus is more supportive of the multi-fault basement model than that of the single main fault (Blackwell et al., 2000). However, the interpretation remains non-unique: although Stillwater Range lithologies were intersected at a depth of ~400 m in well 38-32, near where the step in resistivity to values of 100 ohm-m or more occurs, an unknown amount of slide block material may exist over the main Dixie Valley range-front fault here to complicate the structural framework (Johnson and Hulen, 2002). A particularly low resistivity zone flanks the interpreted main offsetting fault and may be due to alteration from geothermal fluid outflow and upflow. There also is a near-surface concentration of such intersected by well 38-32.

Plans include final editing, formatting, and inversion of the other two lines of array data in Figure 1, through the Cottonwood Canyon and main production area, and through the section 10-15 wells and range-front fumarole. Moreover, when the MT data were acquired, a modified pole-dipole resistivity survey was carried out by the contractor coincident with the MT receiving bipoles as a complementary galvanic electrical data set to help improve resolution. This data set will be combined with the MT in a formal joint inversion to yield final resistivity sections. Key features to be sought in the other model sections include shallow high resistivities persisting (or not) well southeastward from the topographic scarp, and concentrated low resistivity zones projecting surfaceward along the main Dixie Valley offsetting fault which may represent concentrations of upflow and alteration. Resistivity structure will be correlated with possible igneous reservoir rocks, fault zones and offsets, and zones of possible fluidization along fault zones using constraints from pre-existing structural mapping, reflection seismic surveying, drilling, and thermal modeling.

Acknowledgements

The data acquisition of this project was supported under U. S. Dept. of Energy contract DE-FG07-02ID14416, while development of MT inversion technology was supported by contract DE-FG07-00ID13891. The author is indebted to Jon Powell and Bill Doerner of Quantec Geoscience Ltd for their diligence in acquiring high quality array data. Many useful discussions on the Dixie Valley thermal area were carried out with colleagues Jeff Hulen and Pete Rose of EGI.

References

- Barton, C. A., Hickman, S., Morin, R., Zoback, M. D., and Benoit, D., 1998, Reservoir scale fracture permeability in the Dixie Valley, Nevada, geothermal field: Proc. 23rd Workshop on Geothermal Reservoir Engineering, Stanford University, Stanford.
- Bennett, R. A., Wernicke, B. P., Niemi, N. A., Friedrich, A. M., and Davis, J. L., 2003, Contemporary strain rates in the northern Basin and Range province from GPS data: *Tectonics*, 22, doi: 10.1029/TC001355.
- Benoit, R., 1999, Conceptual models of the Dixie Valley, Nevada geothermal system: *Geotherm. Resour. Coun. Trans.*, 23, 505-511.
- Blackwell, D. D., Benoit, D., Golan, B., and Wisian, K. W., 1999, Structure of the Dixie Valley geothermal system, a “typical” Basin and Range geothermal system: *Geotherm. Resour. Coun. Trans.*, 23, 525-531.
- Blackwell, D. D., Golan, B., and Benoit, D., 2000, Thermal regime in the Dixie Valley geothermal system: Proc. World Geothermal Congr., Kyushu, Japan, 991-996.
- Christiansen, R. L., and R. S. Yeats, 1992, Post-Laramide geology of the U. S. Cordilleran region: *in* Burchfiel, B. C., Lipman, P. W., and Zoback, M. L., eds., *The Cordilleran orogen: coterminous U. S.: The Geology of North America*, G-3, Geol. Soc. Amer., Boulder, 261-406.
- DeGroot-Hedlin, C. D., and Constable, S. C., 1990, Occam’s inversion to generate smooth, two-dimensional models from magnetotelluric data: *Geophysics*, 93, 1613-1624.
- DeLugao, P. P., and Wannamaker, P. E., 1996, Calculating the two-dimensional magnetotelluric Jacobian in finite elements using reciprocity: *Geophys. J. Int.*, 127, 806-810.
- Dilek, Y., and Moores, E. M., 1995, Geology of the Humboldt igneous complex, Nevada, and tectonic implications for the Jurassic magmatism in the Cordilleran orogen: *in* Miller, D. M., and C. Busby, eds., *Jurassic magmatism and tectonics of the North American Cordillera*, GSA Spec. Pap. 299, 229-248.
- Egbert, G. D., and Booker, J. R., 1986, Robust estimation of geomagnetic transfer functions: *Geophys. J. Roy. Astr. Soc.*, 87, 173-194.
- Hickman, S., M. J. Zoback, and R. Benoit, 1998, Tectonic controls on reservoir permeability in the Dixie Valley, Nevada, geothermal field: Proc. 23rd Workshop on Geothermal Reservoir Engineering, Stanford University, Stanford.
- Johnson, S. D., and Hulen, J. B., 2002, Subsurface stratigraphy, structure, and alteration in the Senator thermal area, northern Dixie Valley geothermal field, Nevada – initial results from injection well 38-32, and a new structural scenario for the Stillwater escarpment: *Geotherm. Resour. Coun. Trans.*, 26, 533-542.
- Larsen, J. C., Mackie, R. L., Manzella, A., Fiordelisi, A., and Rieven, S., 1996, Robust smooth magnetotelluric transfer functions: *Geophys. J. Int.*, 124, 801-819.
- Okaya, D. A., and Thompson, G. A., 1985, Geometry of Cenozoic extensional faulting: Dixie Valley, Nevada: *Tectonics*, 4, 107-125.
- Pellerin, L., and Hohmann, G. W., 1990, Transient electromagnetic inversion: a remedy for magnetotelluric static shifts: *Geophysics*, 55, 1242-1250.
- Plank, G. R., 1999, Structure, stratigraphy and tectonics of a part of the Stillwater escarpment and implications for the Dixie Valley geothermal system: M.S. thesis, Univ. of Nevada, Reno.
- Rodi, W. L., and Mackie, R. L., Nonlinear conjugate gradients algorithm for 2-D magnetotelluric

Wannamaker

- inversion: *Geophysics*, 66, 174-187, 2001.
- Smith, R. P., Wisian, K. W., and Blackwell, D. D., 2001, Geologic and geophysical evidence for intra-basin and footwall faulting at Dixie Valley, Nevada: *Geotherm. Resour. Counc. Trans.* 25, 323-326.
- Speed, R. C., 1976, *Geology of the Humboldt lopolith and vicinity*: Geol. Soc. Amer. Map MC-14, Boulder, CO.
- Tarantola, A., 1987, *Inverse problem theory*, Elsevier, New York, 671 pp.
- Torres-Verdin, C., and Bostick, F. X., 1992, Principles of spatial surface electric field filtering in magnetotellurics: electro-magnetic array profiling (EMAP): *Geophysics*, 57, 603-622.
- Waibel, A. F., 1987, An overview of the geology and secondary mineralogy of the high temperature geothermal system in Dixie Valley, Nevada: *Geotherm. Resour. Counc. Trans.*, Sept., p. 5-11.
- Wannamaker, P. E., 1999, Affordable magnetotellurics: interpretation in natural environments, in *Three-dimensional electromagnetics*, ed. by M. Oristaglio and B. Spies, *Geophys. Devel. Ser.*, 7, Soc. Explor. Geophys., Tulsa, 349-374.
- Wannamaker, P. E., Doerner, W. M., Stodt, J. A., and Johnston, J. M., 1997, Subdued state of tectonism of the Great Basin interior relative to its eastern margin based on deep resistivity structure: *Earth Planet. Sci. Lett.*, 150, 41-53.
- Ward, S. H., et al., 1978, A summary of the geology, geochemistry and geophysics of the Roosevelt Hot Springs thermal area, Utah: *Geophysics*, 43, 1515-1542.
- Welhan, J. A., Poreda, R. J., Rison, W., and Craig, H., 1988, Helium isotopes in geothermal and volcanic gases of the western United States, 1. regional variability and magmatic origin: *Bull. Volc. Geotherm. Res.*, 34, 185-199.

Figures

Figure 1. Simplified geological map of the Dixie Valley (DV)-Stillwater Range (SR) area surrounding the Dixie Valley thermal field. Black lines show acquired contiguous MT/DC profiling through the system and adjacent fumarole fields. Lines are labeled N (north), C (central) and S (southern). Original figure courtesy Jeff Hulen.

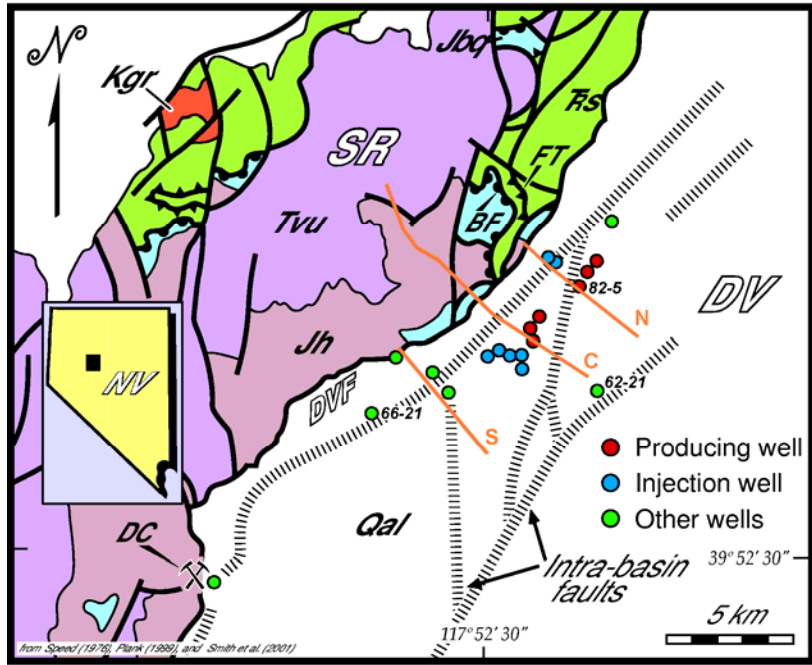
Figure 2. Left: fault splay model of the Dixie Valley/Stillwater Range bounding structure compared to the single fault model (Blackwell et al., 1999). Right: cross section of Dixie Valley in the southern lease area based on the two fault interpretation (Blackwell et al., 2000). Graphics courtesy of Dave Blackwell.

Figure 3. Pseudosections of apparent resistivity (ρ) and impedance phase (ϕ) for 60 MT soundings across the Senator fumaroles and northwestern Dixie Valley. Nominal TE mode is xy and nominal TM mode is yx. The x-axis is assigned to presumed average strike of N40°E, and y is orthogonal to the southeast.

Figure 4. Electrical resistivity section for the northern (N) profile of Figure 1 derived from 60 array MT sites taken with contiguous, 100 m long electric field bipoles. Tick marks are located at bipole centers. Bedrock-alluvium interface is interpreted to lie near the 70-100 ohm-m “contour”.

Wannamaker

Senator fumeroles are denoted SF, and wells 38-32 and 82-5 are projected onto section.



DIXIE VALLEY GEOTHERMAL SYSTEM

Lithologic units abbreviated as —

- Jh* - Jurassic Humboldt igneous complex
- Jbq* - Jurassic Boyer Ranch Formation quartzite
- Kgr* - Cretaceous granite
- Qal* - Quaternary alluvium, colluvium, and lacustrine sediments, undivided
- FtS* - Triassic metasedimentary rocks
- Tvu* - Tertiary volcanic rocks, undivided

Other abbreviations —

- BF* - Boyer fault
- DC* - Dixie Comstock mine and precious-metal deposit
- DVF* - Dixie Valley fault (zone)
- FT* - Fencemaker thrust

Figure 1.

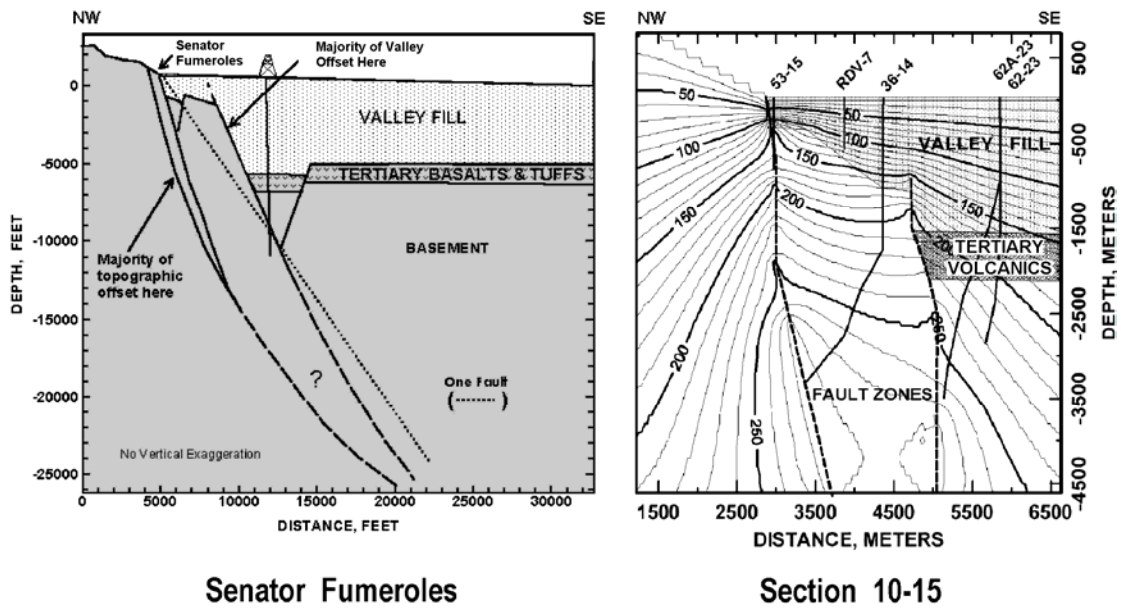


Figure 2.

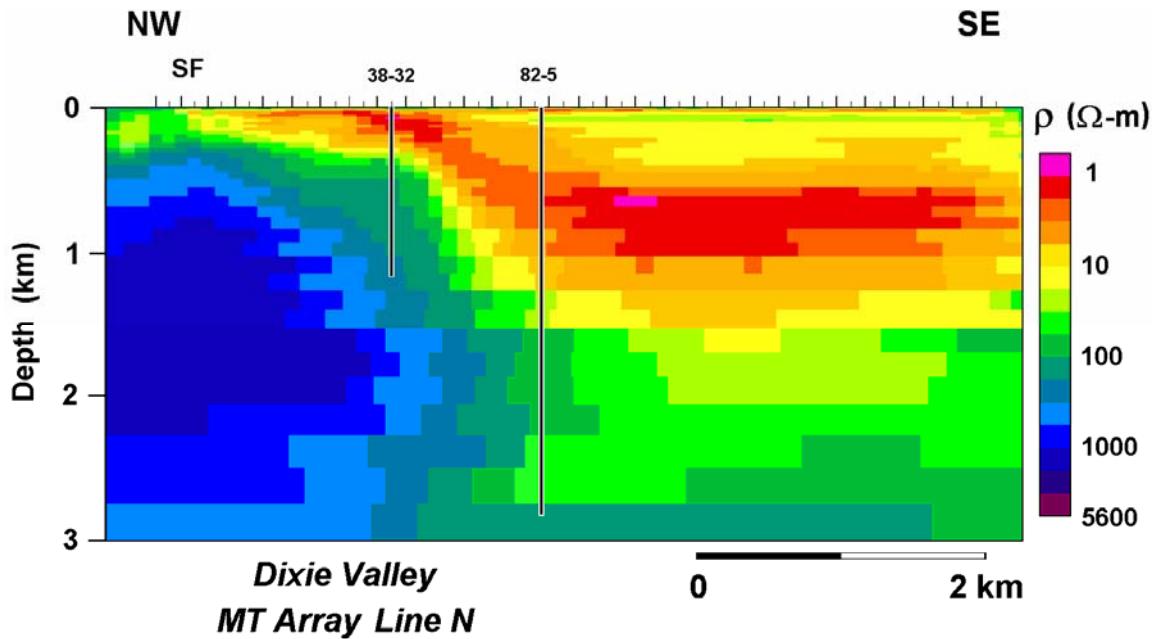
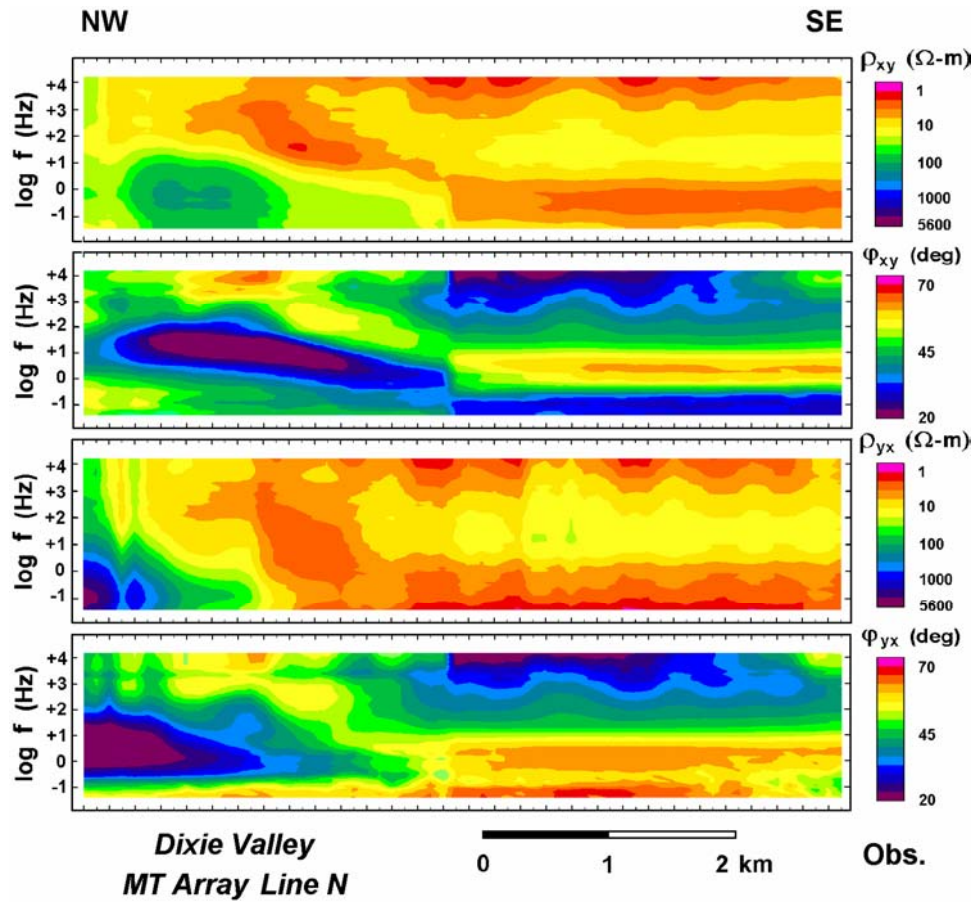


Figure 3.
Figure 4.

